The Structural Response of the Compliant Lung to Different Ventilation Volumes Assessed by Multiple Exchange Time Xenon Transfer Contrast (MXTC)

I. Dregely[1], I. C. Ruset[2], J. Ketel[2], S. Ketel[2], J. F. Mata[3], T. A. Altes[3], G. W. Miller[3], J. P. Mugler III[3], F. W. Hersman[1,2], and K. Ruppert[3]
[1]Physics, University of New Hampshire, Durham, NH, United States, [2]Xemed LLC, Durham, NH, United States, [3]Radiology, University of Virginia, Charlottesville, VA, United States

Introduction: Xenon polarization Transfer Contrast (XTC) MRI is a method that measures lung function by monitoring the decay of the hyperpolarized xenon-129 (HXe129) magnetization in alveolar air spaces (gas phase) due to gas exchange after the application of a series of RF pulses centered at the resonance frequency of HXe129 dissolved in the lung parenchyma (dissolved phase) [1,2]. By varying the delay time between these RF pulses one can control whether only xenon atoms in the septal walls close to the surface are permitted to exchange or whether xenon atoms from the wall interior are included as well. In this work we use 3D multiple-exchange time XTC (MXTC) to measure the gas phase depolarization for several different delay times, which allows the extraction of the xenon gas exchange time constant as well as information about the volume of the dissolved phase compartment. We employed 3D MXTC to investigate the lung structure in rabbits at two different ventilation volumes.

Methods: Experiments were performed on a 1.5 T commercial whole-body imager (Avanto, Siemens Medical Solutions) using a custom-made transmit-receive birdcage RF coil (IGC Medical Advances, Milwaukee, WI). The three imaging segments of the XTC acquisition were 3D FLASH sequences with excitation flip angles of 2°, 2° and 4°. The following sequence parameters were used: non-selective excitation with 500 µs rectangular RF pulses; matrix size 12x28x32; TR/TE 6/3 ms; FOV 108 mm; receiver bandwidth 260 Hz/pixel. The FLASH image acquisitions were separated by a series of contrast generating 90° 1 ms Gaussian RF pulses, with an inter-pulse delay ranging from 5 ms to 80 ms, applied at the dissolved phase resonance frequency of 202 ppm for the XTC experiments or at -202 ppm for the control experiment. Two New Zealand rabbits (approximately 5 kg) were used. Each animal was anesthetized with a mixture of Xylazine 5 mg/kg and Ketamine 50 mg/kg, intubated and placed in the xenon RF coil. Immediately before the pulse sequence was started the animal was ventilated alternately with 20 cc (low volume) or 40 cc (high volume) of isotopically enriched xenon gas (~87% xenon-129), which was polarized to approximately 35% using a commercial prototype polarizer (Xemed LLC, Durham NH). The protocol was approved by our Institutional Animal Care and Use Committee.

The resulting 3D MXTC maps were fitted on a voxel-by-voxel basis to the first-order term of a simple diffusion model [1,3]: $f_D = \lambda V_t/V_a \cdot \left(1 - \frac{8}{\pi^2}\exp\left(-\tau/\tau_c\right)\right)$, where f_D is the gas depolarization per 90° pulse, λ is the Ostwald solubility, V_t/V_a is the ratio of tissue and alveolar volume, τ is the delay time and τ_c is the exchange time constant.

Results: Maps of the fitting results for the maximum depolarization and the time constant for the two ventilation volumes in one rabbit are shown in Figure 1. The mean values for each slice are plotted in Figure 2. For the low lung volume the maximum depolarization (Figure 2a, red), which is proportional to the tissue-to-alveolar volume, increased from anterior to posterior slices. This observation is consistent with the clinical observation that the tissue density of the lung on CT is greater in the dependent portions of the lung, the so called slinky effect [4,5]. Alveoli in the dependent regions of the lung are less inflated and therefore smaller, resulting in an increased maximum depolarization as measured by MXTC. For high volumes (40cc, which is beyond total lung capacity for rabbits), the high gas pressure balances the tissue weight and the anterior-posterior gradient disappears (Figure 2a, blue). The two curves intersect such that for the most anterior slice at low ventilation volume the maximum depolarization drops below the one for high volume ventilation. This can be understood with the help of the slinky model as a stretching and thinning of the alveolar walls by the weight of the lung tissue. This argument is further supported by the posterior to anterior drop of the exchange time constant τ_c for the low ventilation volume (Figure 2b, red). Since $\tau_c \propto \sqrt{L}$, where L is the thickness of the alveolar wall, the wall in the anterior partitions appears to be thinner than in the posterior lung due to stretching. When the rabbit is ventilated with higher volumes (Figure 2b, blue) the effect of the gravitational pull diminishes as the ventilation pressure increases and the tissue thickness becomes more homogeneous.

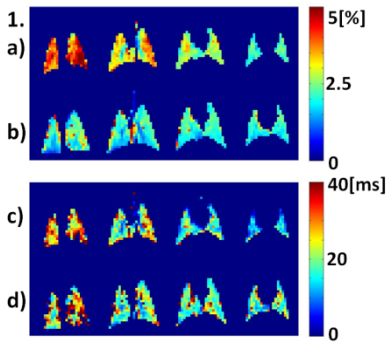

Figure 1: Fitted gas-exchange parameters for four partitions: Maximum depolarization at a) low and b) high ventilation volume; exchange time constant at c) low d) high ventilation volume.

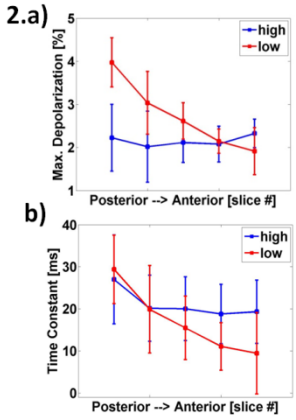

Figure 2: Average maximum depolarization (a) and exchange time constant (b) in five partitions (from most posterior to most anterior) at high (blue) and low (red) ventilation volumes.

Conclusion: 3D MXTC permits the regional assessment of the septal wall thickness and the tissue-to-alveolar-volume ratio. We investigated the response of the rabbit lung to variations of the ventilation volume and found the slinky model to be an adequate description of the underlying structural physiology.

References: **[1]** Ruppert K, Mata JF, Brookeman JR, Hagspiel KD, Driehuys B, Mugler III JP. MRM 2004; 51(4):676-87. **[2]** Patz, S.; Muradian, I.; Hrovat, M. I.; Ruset, I. C.; Topulos, G.; Covrig, S. D.; Frederick, E.; Hatabu, H.; Hersman, F. W. & Butler, J. P. Acad Rad 2008; 15(6):713-727. **[3]** Månsson, S.; Wolber, J.; Driehuys, B.; Wollmer, P. & Golman, K. MRM 2003; 50(6): 1170-1179. **[4]** Hopkins, S. R.; Henderson, A. C.; Levin, D. L.; Yamada, K.; Arai, T.; Buxton, R. B. & Prisk, G. K. JAP 2007: 103(1),:240-248. **[5]** West JB, Matthews FL, JAP 1972; 32:332-345.

Acknowledgements: Supported by NIH grants R01 EB003202, R42 HL082013 and R01 HL079077, the New Hampshire Innovation Research Center and Siemens Medical Solutions.